Geochemical characteristics and tectonic implications of HP-UHP eclogites and blueschists in southwestern Tianshan, China*

AI Yongliang[1], ZHANG Lifei[1]**, LI Xuping[2] and QU Junfeng[1]

(1. MOE Key Laboratory of Orogenic Belt and Crust Evolution, School of Earth and Space Sciences, Peking University, Beijing 100871, China; 2. School of Geosciences and Resources, China University of Geosciences, Beijing 100083, China)

Received July 18, 2005; revised December 23, 2005

Abstract Four rock assemblages in correspondence with two different tectonic settings have been recognized in the NEE-SWW extending HP-UHP metamorphic belt in southwestern Tianshan, northwest China. Eclogite assemblage EC1 is geochemically akin to alkaline within-plate oceanic island basalt (OIB). EC2 shows affinity to enriched mid-oceanic ridge basalt (EMORB). Rare earth element (REE) and other immobile trace element characteristics of blueschist assemblage BS1 resemble those of normal mid-oceanic ridge basalt (NMORB). These three assemblages are likely formed on a seamount setting, and the prevalent presence of carbonate minerals and omphacite quartzite stripes/gobbets suggests ancient pelagic sediments including marls are probably developed upon the basaltic seamount. Whereas the geochemical characteristics of BS2 assemblage are of volcanic arc basalt-type. The seamount with the pelagic sediments on it is brought into the subduction zone, and volcanic arc basalts formed on the active continental margin and trench sediments are eroded and enwrapped in the subducting mass, they are altogether subjected to high to ultrahigh pressure metamorphism and subsequent exhumation towards surface. The HP-UHP metamorphic belt is thus interpreted as a subduction-accretionary complex formed by tectonic juxtaposition and imbrication of seamount, seafloor, trench and volcanic arc sequences during oceanic crust subduction.

Keywords: southwestern Tianshan, HP-UHP metamorphic belt, subduction-accretion complex, trace element geochemistry.

Since the discovery of the eclogites at the upper streams of Akyazi River in southwestern Tianshan, Xinjiang[1], some previous work has primarily established the tectonic frame of the study area[2,3]. The eclogites and the related blueschists are considered to be components of the accretionary wedge formed in the subduction of the southern Tianshan oceanic crust under the active continental margin of Yili-central Tianshan plate and its subsequent exhumation. Ultrahigh pressure (UHP) metamorphosed minerals/mineral assemblages have been found in the detailed petrological studies in the past few years, which suggests the eclogite-blueschist belt has probably undergone UHP metamorphism, such as quartz pseudomorphs after coesites in garnets and quartz exsolution lamellae in omphacites[4], residue magnesite of metamorphic genesis[5], the residue coesite exsolution within omphacite grains[6], and the metamorphic reaction of magnesite and aragonite being transformed to dolomite preserved in the paragenetic muscovite schists[7].

Well-preserved pillow lava outershapes of some eclogites and blueschists unveil their ocean floor subduction genesis[8]. The study area has been proved to be the second sea floor composite, after Zermat Saas terrane in western Alps, that has undergone UHP metamorphism and thus aroused much attention of petrologists from worldwide. Nevertheless, the protolith geochemistry and the affirmatory tectonic background of these HP-UHP rock assemblages are left yet to be further studied. The present paper reports the results of major element, trace element, and Sm-Nd isotope analyses of southwestern Tianshan HP-UHP metabasite rock assemblages on the basis of detailed petrological observations, and discusses their probable implications in tectonic evolution.

1 Geological background

Tianshan range is the longest E-W extending mountain range in the world, stretching for about 2500 km lying across Middle Asia. Southern Tianshan orogenic belt is its western branch starting at Uzbekistan in the west and ending at Yili, Xinjiang, China where eastern Tianshan starts. The range represents the subduction and collision belt between Yili-central Tianshan plate and Tarim plate, and formed

* Supported by National Natural Science Foundation of China (Grant Nos. 40325005, 40228003, 40272031), MOE Young University Teachers Award Program and partly by Peking University Analysis Fund

** To whom correspondence should be addressed. E-mail: Lfzhang@pku.edu.cn

in between is the HP-UHP metamorphic belt stretching east-west for about 1500 km, from Fan-karategin of Tajikistan in the west to Atbashi of Kirghizia, to Changawuzi, Akyazi and Keksu in Xinjiang, China in the east. The southwestern Tianshan in Xinjiang is the Chinese part of the southern Tianshan range, stretching east-west between Yili-central Tianshan and Tarim plates for more than 200 km, within which is formed an HP-UHP metamorphosed metabasite rock series represented by eclogites and blueschists[3,8] (Fig. 1). The main component rocks in the HP-UHP belt are eclogites, blueschists, and phengite schists. UHP eclogites have three types of occurrences, and the type I eclogites are preserved as pods, boudins, thin layers, and thick layers in blueschists. The HP-UHP belt is separated by ductile shear zones on the north with Precambrian crystalline basis and on the south with intercalating marbles and chlorite muscovite schists (Fig. 1).

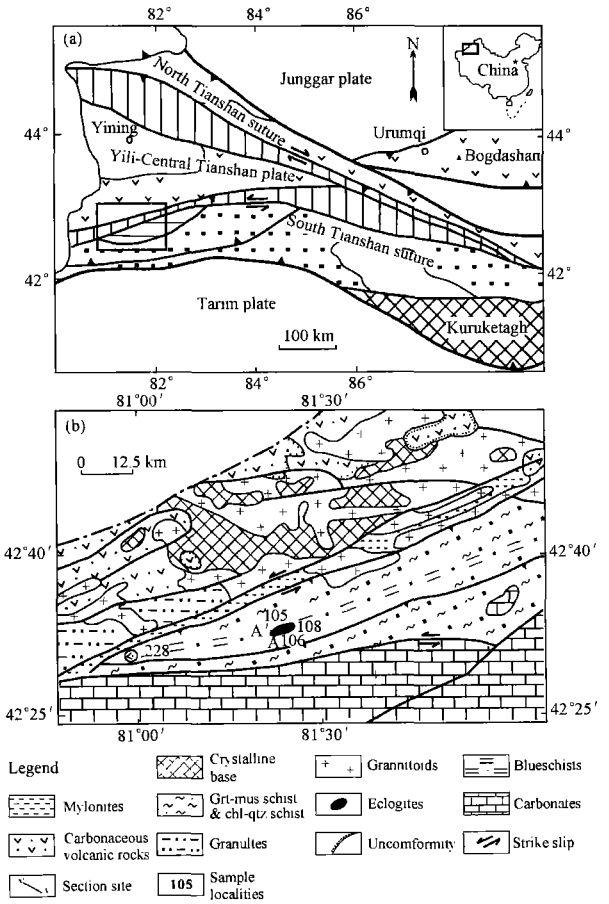

Fig. 1. Schematic tectonic map of the HP-UHP metamorphic belt, southwestern Tianshan, China (modified from [4]) (a) Regional geological map; (b) geological map of study area and sample locations.

A latest study on the southern margin of the Precambrian crystalline basis to the north of the HP-UHP belt has unveiled an HT-LP metamorphic belt characteristic of occurrence of bi-pyroxene granulites and granulite facies metamorphosed cordierite garnet gneisses along Muzart River. The HT-LP belt represents a continental volcanic arc developed upon the southern active margin of Yili-central Tianshan plate during the northward subduction of Tarim plate. This HT belt and the LT eclogite and blueschist belt, formed by residue ophiolite slice via HP-UHP metamorphism, form paired metamorphic belts across the northern ductile shear zone[9]. SHRIMP U-Pb dating results of zircons of eclogites suggest that the HP-UHP belt is probably formed in the period of 232 Ma—225 Ma[10].

2 Petrology

The HP-UHP metabasites discussed herein consist mainly of type I eclogites, garnet blueschists, and chlorite blueschists. The eclogites and blueschists are divided further to four rock assemblages according to their field occurrence and petrology.

Eclogite assemblage EC1 consists mainly of massive eclogites, garnet glaucophane schist stripes/lenses, and occasionally of garnet muscovite schist (sampling site 105 in Fig. 1(b)). UHP minerals such as coesite exsolution stripes[7], coesite pseudomorphs[4] are present in these eclogites. EC2 assemblage consists of intercalating quartz eclogites and lenticular blueschists, garnet phengite schists, with minor omphacite quartzite stripes/gobbets (sampling site 106 in Fig. 1(b)). The eclogites have a mineral paragenesis of garnet, omphacite, phengite, epidote, glaucophane, paragonite, quartz, dolomite, magesite and rutile. The coesite pseudomorphs with radiative cracking within garnets and remnant metamorphosed magnesites[5] are spotted in these rocks. Blueschist assemblage BS1 consists of interlayered garnet blueschists and garnet phengite schists, and intercalated quartzite laminae and lenses. Primary minerals include garnet, glaucophane, zoisite, paragonite, actinolite, epidote, quartz and titanite. BS2 assemblage consists of intercalating thin-layered muscovite chlorite blueschists and garnet muscovite quartz schists. The blueschists are granoschistoblastic or schistoblastic, granular glaucophanes, dolomites, epidotes, quartz, albites and accessory titanites distributing along the schistosity lined up by the schistose phengites, paragonites, and chlorites.

3 Geochemistry

The fresh samples after mechanically peeling off the oxidized surfaces and ultrasonic cleaning were crushed to pieces by corundum crocodile squeezers and subsequently ground into 200 screen mesh in agate jars at the pollution-free lab. Both major and trace elements were analyzed at the Continental Dynamics Lab of Northwest University, Xi'an. Major elements were analyzed on glass pellets (Li-tetraborate flux) using X-ray fluorescence (XRF). Loss on ignition was determined from the weight differential after heating the samples to 800 ℃. Trace elements were analyzed on an ELAN6100DRC ICP-MS of PE Inc. and the parallel analyses of international standard materials BHVO-1, AGV-1, and G-2 showed a precision better than 10% compared to the reference values.

Sm-Nd isotopic measurements were completed by the isotope dilution method on a VD354 solid isotope mass-spectrometer at the Institute of Geology and Geophysics, Chinese Academy of Sciences. Dissolution of the ^{149}Sm-^{150}Nd diluted spiked rock powders (50—100 mg each) was done by $HClO_4$ + HF digestion in sealed teflon vessels for a week at 120 ℃, and recurrent drying at 140 ℃ on hot plane and repeated HCl treatment until complete anion replacement by Cl^-. Pure Sm and Nd concentrates were obtained by passing the solution through AG50W * 8 (H^+) ion exchange resin columns and P507 extracting resin. $^{143}Nd/^{144}Nd$ measurements were normalized to $^{146}Nd/^{144}Nd = 0.721900$. Parallel analyses of La Jolla Nd and BCR-1 standards yielded values of $0.511862 \pm 7(2\sigma, n = 6)$ and $0.512626 \pm 9(2\sigma, n = 2)$ respectively.

The major, trace element compositions and Sm-Nd isotopic compositions of eclogite and blueschist assemblages of southwestern Tianshan HP-UHP belt are listed in Tables 1 and 2 respectively.

The SiO_2 contents of eclogite assemblages and blueschist assemblage BS1 are fairly low (45.3%—50.3%), except for a sample transient with quartize whose SiO_2 content is as high as 54.1%, while BS2 has higher SiO_2 contents (52.89%—53.90%). Most eclogite samples have higher contents of K_2O (0.6%—3.14%), Na_2O (2.29%—5.08 %) and TiO_2 (>2%), much higher than those of blueschist assemblages. Besides, eclogites have Al_2O_3 and P_2O_5 contents higher than BS1 blueschists. Most samples have LOI of 0.71%—3.79%, while those of the BS2 samples are higher than 6.80%, in confirmity with their considerable water- and CO_2-bearing mineral contents. The fluctuation of the Na_2O, K_2O, and MgO contents of the samples in the same assemblage indicates that their protolith compositions have been changed to some extent in seafloor alteration and seafloor metamorphism, dehydration in the subduction zone, and subsequent low-temperature metamorphism after their exhumation onto shallow level[11,12].

The protoliths of rocks of the assemblages would undergo one or more above-mentioned processes and the contents of the water-soluble elements such as Ba, Rb, Cs, U, K, Na, La, Ce, Sr, Pb would be changed to some extent[13] and Th becomes mobile in the extreme condition in the subduction zone, whilst other trace elements such as high field strength elements Nb, Ta, Zr, Hf, Ti, rare earth elements (except for La, Ce), Y, and high compatible element Ni, V, Cr would survive these processes and their contents remain nearly unchanged. Two useful ratios of immobile elements Nb/Y and Zr/Ti are used to substitute for $K_2O + Na_2O$ and SiO_2[14] in the protolith classification and genetic environment discussions of southwestern Tianshan HP-UHP metamorphosed rocks.

As shown in Fig. 2, assemblages EC1 and EC2 are plotted in the alkaline basalt and sub-alkaline basalt fields respectively, and BS1 and BS2 assemblages in the andesitic basalt field.

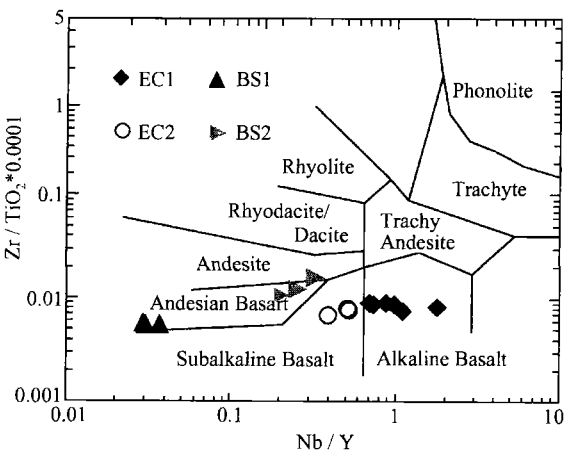

Fig. 2. Trace element classification diagram of southwestern Tianshan HP-UHP rocks (based on [14])

Each assemblage has a specific trace element geochemical signature as is shown in analyses (Fig. 3, Table 1).

Table 1. Major and trace element compositions of the rocks in southwestern Tianshan HP-UHP belt

Assem.	Ec1						Ec2			Bs1			Bs2		
Sample	1051	10512	10512C	10513	10516	1054	10610	10611	1068	1082	1083	1085	2284[a]	2286[a]	2287[a]
Rock type	BS	Ec	Ec	Ec	Ec	BS	BS	Ec	Ec	BS	BS	BS	BS	BS	BS
Major elements (%)															
SiO_2	48.23	49.86	46.28	47.63	48.86	47.28	54.10	45.32	45.91	48.04	46.39	50.35	53.15	53.42	54.20
TiO_2	2.67	2.77	2.80	2.86	2.76	2.72	1.79	2.09	2.13	1.36	1.31	1.42	0.77	1.00	0.78
Al_2O_3	17.06	14.80	15.41	12.80	15.16	16.31	14.60	15.41	15.58	14.10	14.23	13.39	14.29	13.59	11.62
TFe_2O_3	13.94	11.43	11.81	14.20	15.50	13.41	12.51	14.27	12.97	15.08	14.90	13.34	7.99	9.51	8.96
MnO	0.14	0.13	0.15	0.09	0.15	0.18	0.15	0.16	0.06	0.34	0.29	0.23	0.17	0.12	0.18
MgO	3.89	6.90	5.37	4.25	3.38	5.81	5.78	3.68	5.82	6.32	5.58	6.69	10.10	11.80	12.37
CaO	6.15	7.48	8.88	7.36	8.58	8.82	2.18	7.52	8.74	10.56	10.36	10.94	9.17	5.55	7.31
Na_2O	2.58	3.57	4.52	5.08	2.29	3.05	3.37	3.97	3.46	1.78	2.84	2.87	1.55	3.18	2.95
K_2O	2.20	0.90	1.02	2.44	1.26	0.60	3.14	3.07	1.38	0.27	0.09	0.08	2.64	1.68	1.36
P_2O_5	0.66	0.45	0.48	0.22	0.56	0.36	0.22	0.23	0.16	0.09	0.11	0.11	0.17	0.16	0.27
LOI	2.03	1.51	3.22	3.32	1.17	1.10	2.19	3.79	3.57	1.78	3.50	0.71	0.00	0.00	0.00
TOTAL	99.55	99.80	99.94	100.25	99.67	99.64	100.03	99.51	99.78	99.72	99.60	100.13	100.00	100.00	100.00
Trace elements ($\times 10^{-6}$)															
V	210.95	219.97	295.66	266.94	238.43	219.85	139.79	245.79	311.67	383.76	349.29	411.64	146.24	174.12	153.42
Cr	98.15	143.85	146.29	113.19	126.50	107.32	127.63	137.18	143.55	105.73	162.97	120.58	305.82	539.15	739.23
Ni	59.44	111.13	86.28	45.27	37.65	108.16	77.78	59.52	130.82	55.72	63.29	56.75	233.61	376.92	442.21
Rb	46.76	13.89	19.80	57.79	28.90	11.38	66.71	88.67	38.92	8.15	2.28	1.44	81.56	46.88	37.72
Sr	259.52	281.41	219.84	117.43	182.14	464.12	55.53	143.79	212.89	133.84	143.84	93.10	281.64	123.97	118.19
Y	40.16	29.47	34.74	21.55	45.54	38.85	32.09	33.53	24.75	42.67	41.42	36.14	22.77	24.46	25.33
Zr	242.71	244.82	216.42	238.73	250.99	236.62	141.13	174.69	149.39	78.65	74.44	79.97	125.35	134.38	69.37
Nb	27.95	29.26	38.16	39.06	40.32	28.66	16.39	17.63	9.62	1.25	1.25	1.35	7.44	6.54	4.82
Ba	787.10	659.17	171.84	442.88	299.70	227.12	374.85	392.02	286.06	90.13	24.40	17.85	1388.64	1153.91	945.87
La	25.61	26.93	31.66	26.57	26.00	24.81	17.66	13.57	11.74	1.97	2.07	2.57	18.37	12.86	13.18
Ce	56.99	58.88	66.62	56.70	54.23	56.04	40.37	32.99	30.07	6.61	6.86	8.39	37.71	26.75	24.98
Pr	7.16	7.57	8.70	7.12	6.71	7.19	5.35	4.29	4.44	1.19	1.23	1.49	4.60	3.44	3.46
Nd	30.06	32.74	37.09	29.95	27.65	31.70	23.77	19.29	21.87	7.19	7.25	8.57	17.86	14.18	15.00
Sm	6.65	7.58	8.14	6.64	6.04	7.48	5.90	4.73	6.20	2.89	2.81	3.22	3.65	3.32	3.71
Eu	2.08	2.18	2.50	1.96	1.97	2.24	1.74	1.49	2.11	1.05	1.01	1.15	0.99	1.01	1.09
Gd	7.02	6.64	7.99	5.91	7.11	7.46	5.76	4.69	5.99	4.06	3.92	4.04	3.68	3.66	4.03
Tb	1.21	1.02	1.18	0.82	1.31	1.24	0.98	0.85	0.89	0.91	0.90	0.83	0.59	0.64	0.68
Dy	6.98	5.43	6.33	4.17	7.34	6.85	5.67	5.28	4.51	6.11	5.91	5.40	3.47	3.76	3.93
Ho	1.43	1.04	1.23	0.76	1.52	1.37	1.20	1.17	0.87	1.46	1.42	1.23	0.75	0.83	0.86
Er	3.60	2.61	3.17	1.93	3.78	3.41	3.12	3.36	2.32	3.99	3.89	3.43	2.09	2.23	2.26
Tm	0.52	0.38	0.46	0.27	0.57	0.48	0.47	0.55	0.36	0.65	0.63	0.55	0.33	0.34	0.34
Yb	3.19	2.36	2.93	1.79	3.66	2.98	2.84	3.60	2.38	4.35	4.14	3.60	2.24	2.22	2.17
Lu	0.48	0.35	0.45	0.27	0.57	0.45	0.41	0.55	0.37	0.72	0.67	0.57	0.36	0.35	0.33
Hf	5.47	5.45	5.66	5.18	5.52	5.44	3.28	3.80	3.30	2.13	2.01	2.10	3.04	3.26	1.75
Ta	1.76	1.81	2.47	2.34	2.46	1.80	0.99	1.09	0.62	0.09	0.09	0.09	0.58	0.43	0.31
Pb	2.56	2.89	2.17	1.83	2.14	3.19	1.58	1.98	1.96	4.67	3.79	1.46	9.27	5.32	4.40
Th	3.15	3.09	3.73	3.89	3.60	2.46	2.20	1.49	0.75	0.14	0.14	0.16	7.11	3.77	2.78
U	0.55	0.72	0.86	0.65	0.70	0.66	0.38	0.25	0.15	0.07	0.05	0.05	1.72	1.16	0.87
ΣREE	193.14	185.17	213.19	166.42	193.98	192.55	147.33	129.94	118.87	85.85	84.13	81.20	119.47	100.06	101.34
Σce	128.55	135.88	154.72	128.94	122.59	129.45	94.79	76.36	76.42	20.91	21.22	25.39	83.18	61.56	61.41
ΣY	64.59	49.29	58.47	37.48	71.39	63.10	52.54	53.57	42.44	64.93	62.91	55.81	36.29	38.49	39.93
$(La/Yb)_N$	5.76	8.17	7.75	10.65	5.09	5.96	4.46	2.71	3.53	0.32	0.36	0.51	5.88	4.15	4.35
Eu/Eu^*	0.93	0.94	0.95	0.96	0.92	0.92	0.91	0.97	1.06	0.94	0.93	0.97	0.82	0.89	0.86

[a] Normalized on a no LOI basis

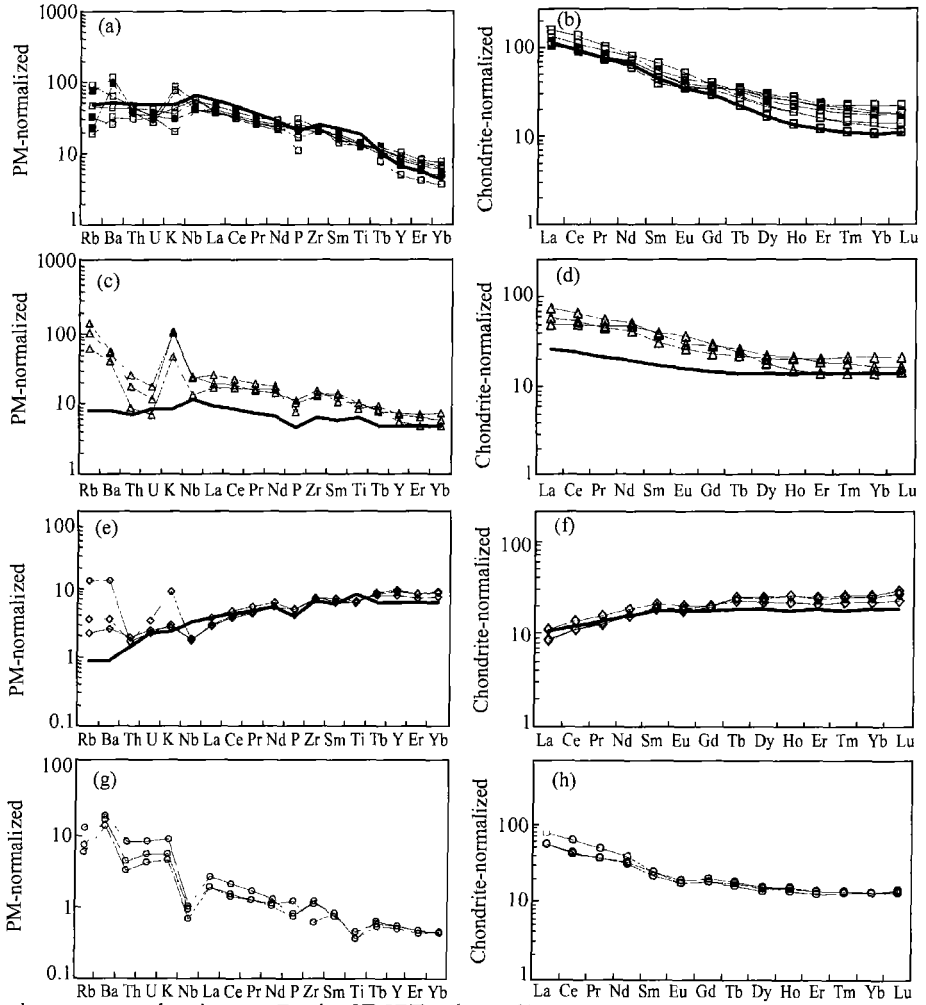

Fig. 3. Trace element patterns of southwestern Tianshan HP-UHP rock assemblages. Normalizing values of primary mantle PM and chondrite C1 are from[15], bold lines in (a) and (b), (c) and (d), (e) and (f) represent OIB, EMORB and NMORB values respectively.[15]

Assemblage EC1 has high REE contents, ΣREE $= 166.4 \times 10^{-6}$—205.6×10^{-6}. LREEs are highly enriched and fractionated, ΣCe/ΣY = 1.72—3.44, $(La/Yb)_N = 5.09$—10.65, $(La/Sm)_N = 2.12$—2.78 and La contents are 105—134 times that of chondrite. While HREEs are relatively flat: average $(Gd/Yb)_N = 2$. No evident Eu anomalies are observed, $Eu/Eu^* = 0.92$—0.97. Zr/Hf = 43.53—46.12 (except for T10512C = 38.22), Nb/La = 1.09—1.55 (except for T1053 = 0.89), and Nb = 25.21×10^{-6}—40.32×10^{-6} ($> 8 \times 10^{-6}$), all close to average OIB[15] (Table 1; Fig. 3(a), (b)). The ratio of $^{143}Nd/^{144}$ Nd varies between 0.512430 ± 7—0.512459 ± 12, $\varepsilon_{Nd}(t) = -1.1$—$-0.1$ (Table 2; Fig. 4(a), (b)). Relative depletion of Sr and enrichment of Pb in some samples probably attribute to the dehydration in subduction and/or minor sediment mixture into them.

EC2 assemblage is also LREE enriched, ΣCe/ΣY = 1.43—1.80, $(La/Yb)_N = 2.71$—4.46. LREE are moderately fractionated, $(La/Sm)_N = 1.22$—1.93. No obvious Eu anomalies are observed, $Eu/Eu^* = 0.91$—1.06. Zr/Hf = 42.97—45.21, Nb/La = 0.73—1.30, and Nb = 9.62×10^{-6}—22.00×10^{-6} ($> 8 \times 10^{-6}$), showing resemblance to E-MORB-type basalts[16] (Table 1; Fig. 3(c), (d)). $^{143}Nd/^{144}Nd$ varies between 0.512388 ± 10—0.512737 ± 11, $\varepsilon_{Nd}(t) = -1.1$—$-0.1$ (Table 2; Fig. 4(a), (b)). Nb contents are considerably lower comparative to those of EC1, which suggests low Nb concentration in their provenance and/or addition of minor marine sediments. The relative depletion of Sr, Th, and U is likely due to the dehydration in subduction.

Table 2. Results of whole-rock Sm-Nd isotopic analyses

Sample	^{147}Sm ($nmol \cdot g^{-1}$)	Sm ($\times 10^{-6}$)	^{144}Nd ($nmol \cdot g^{-1}$)	Nd ($\times 10^{-6}$)	$^{147}Sm/^{144}Nd$	$^{143}Nd/^{144}Nd$ (2σ)	ε_{Nd} (means)	$f_{Sm/Nd}$	Age (Ma)[a]	$\varepsilon_{Nd}(t)$
105-13	6.960	6.979	50.89	30.89	0.1368	0.512459±12	−3.49	−0.30	439	−0.13
105-16	6.220	6.237	46.36	28.14	0.1342	0.512445±5	−3.76	−0.32	439	−0.26
105-4	7.271	7.291	50.29	30.53	0.1446	0.512430±7	−4.06	−0.26	439	−1.14
106-10	5.293	5.308	35.12	21.32	0.1507	0.512388±10	−4.88	−0.23	439	−2.30
106-11	5.087	5.101	33.94	20.60	0.1499	0.512621±11	−0.33	−0.24	439	+2.30
106-8	6.532	6.549	37.93	23.03	0.1722	0.512737±11	1.93	−0.12	439	+3.30
108-2	3.256	3.265	13.02	7.90	0.2501	0.513120±10	9.40	0.27	439	+6.41
108-3	2.871	2.879	11.95	7.25	0.2403	0.513099±11	8.99	0.22	439	+6.55
108-5	3.720	3.73	16.25	9.87	0.2289	0.513103±13	9.07	0.16	439	+8.15
228-4	7.539	7.559	58.33	35.41	0.1292	0.512118±9	−10.14	−0.34	439	−6.36
228-6	3.596	3.606	24.83	15.07	0.1448	0.512279±13	−7.00	−0.26	439	−4.10
228-7	4.349	4.361	29.28	17.77	0.1485	0.512331±10	−5.99	−0.25	439	−3.29

All $^{143}Nd/^{144}Nd$ relative to La Jolla = 0.511862; external precisions: ±0.000020 for $^{143}Nd/^{144}Nd$, 0.2% for $^{147}Sm/^{144}Nd$; ε_{Nd}(meas) is calculated relative to CHUR = 0.512638

[a] Unpublished zircon SHRIMP dating results

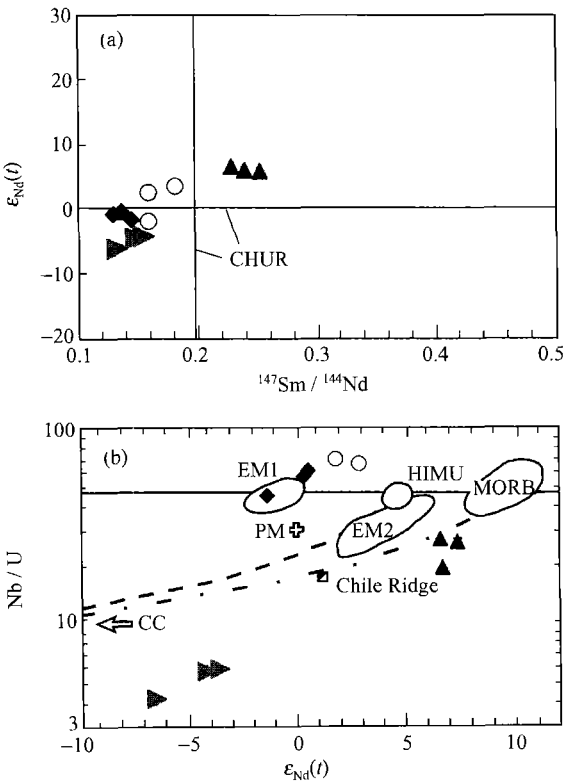

Fig. 4. Sm-Nd isotopic diagrams of southwestern Tianshan HP-UHP rocks. (a) $^{147}Sm/^{144}Nd$-$\varepsilon_{Nd}(t)$ diagram; (b) Nb/U-$\varepsilon_{Nd}(t)$ diagram (based on[19]); (Legends are the same as those in Fig. 2)

Assemblage BS1 is very low in REE contents, $\Sigma REE = 81 \times 10^{-6}$—$86 \times 10^{-6}$, and highly depleted of LREE, La/Yb = 0.3—0.5, $(La/Sm)_N$ = 0.44—0.52, both are obviously below 1. La/Chondrite = 8—11. Left-inclined REE and relatively flat HREE patterns, average $(Gd/Yb)_N$ = 0.76, Zr/Hf = 36.96—38.11 indicate that they are of NMORB provenance. Lower Nb/La (0.53—0.63), Nb = 1.25×10^{-6}—1.35×10^{-6}, less than average NMORB[15] (Table 1; Fig. 3(e), (f)) and higher Pb contents all suggest a certain amount of marine sediment addition. $^{143}Nd/^{144}Nd$ varies between 0.513099 ± 11—0.513120 ± 10, $\varepsilon_{Nd}(t)$ = +6.4—+8.2 (Table 2; Fig. 4(a), (b)).

Assemblage BS2 is typical of strongly right-inclined REE pattern and depleted of all HFSEs: Nb/La = 0.41—0.66, Nb = 3.16×10^{-6}—7.44×10^{-6} ($< 11 \times 10^{-6}$), but enriched in Pb and most LFSEs like Rb, Ba, U, K, which alleges their volcanic arc basaltic (VAB) provenance. Ce/Pb ratio is lower and Ba/La, K/Ta ratios higher compared to those of NMORB: Ce/Pb = 4—6, Ba/La = 72—90, K/Ta = 32020—37572. Their much lower Nb contents and $\varepsilon_{Nd}(t)$ (−6.4 to −3.3; Table 2; Fig. 4) suggest that both subducted oceanic crust derived fluid and continental sediment endmembers have been involved in[17], therefore they are probably of continental arc basalt (CAB) provenance.

4 Protolithic genesis and tectonic implications

The protoliths of the four assemblages of southwestern Tianshan UHP eclogites and the related blueschists correlate with OIB, EMORB, NMORB, and VAB respectively at first glance at their specific major and trace element patterns. Moreover, the HFSE and some other immobile elements may help to reveal the protolithic geneses and tectonic settings.

Nb-Zr diagram indicates that all assemblage plots gather in the specific areas (Fig. 5(d)). In Ti-Zr-Y diagram (Fig. 5(a)), EC1 and EC2 sample plots fall into within-plate basalt (WPB) area, two BS2 samples into calc-alkaline basalt (CAB) area, BS1 samples and one BS2 sample into the mingled area of CAB, MORB and island arc tholeiites (IAT), while in Ti-Zr diagram (Fig. 5(f)), BS1 and BS2 assemblage plots fall definitely into MORB and VAB fields respectively. In Nb-Zr-Y diagram (Fig. 5(c)), EC1 samples are plotted in within-plate alkaline (WPA) and within-plate tholeiite (WPT) fields, EC2 samples plotted within the mingled area of EMORB, VAB, and WPT. The BS2 samples falling into VAB in Fig. 5(c) and the mingled area in Fig. 5(a) are plotted definitely within the CAB field in Hf-Th-Nb diagram (Fig. 5(e)). As Th becomes mobile only under the extreme condition as in the dehydrating process of subducting slab, the BS2 samples falling into the field with low Hf/Th (Fig. 5(e)) are probably formed in supra-subduction zone (SSZ) setting. In

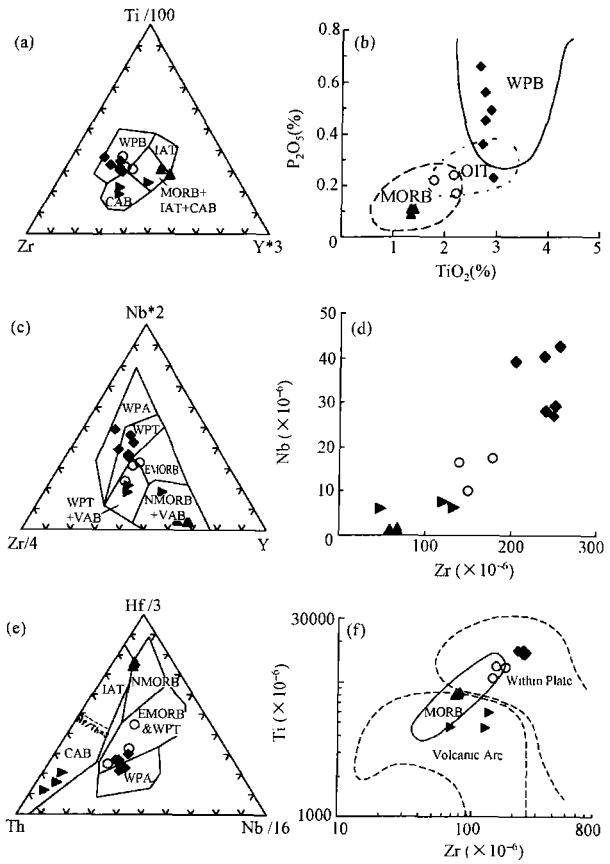

Fig. 5. Trace element ratio diagrams of southwestern Tianshan HP-UHP rocks. (a) Ti-Zr-Y diagram; (b) Ti-P diagram; (c) Nb-Zr-Y diagram; (d) Nb-Zr diagram; (e) Th-Hf-Nb diagram; (f) Ti-Zr diagram (Legends are the same as those in Fig. 2).

Nb, Ti, Nd, Y vs Zr diagram (Fig. 6), EC1 plots fall into the OIB field, BS1 into MORB field, and EC2 into the transient field of the two. The major element Ti-P diagram (Fig. 5(b)) also suggests the close correlation between EC1 and OIB, BS1 and MORB basalts.

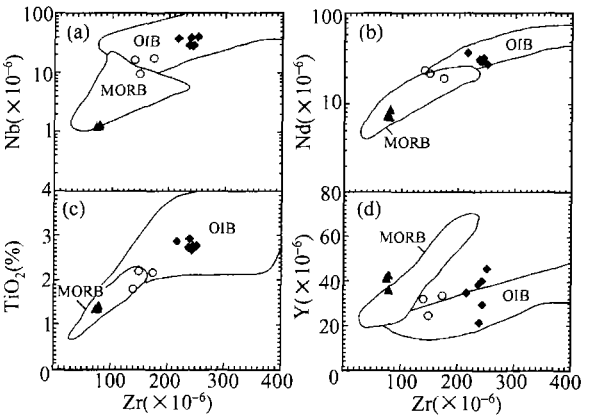

Fig. 6. Nb, Ti, Nd, Y vs Zr diagrams of southwestern Tianshan HP-UHP rocks. (a) Nb-Zr diagram; (b) Nd-Zr diagram; (c) Ti-Zr diagram; (d) Y-Zr diagram (Legends are the same as those in Fig. 2).

Whole-rock Sm-Nd isotopic analyses (Table 2) and $^{147}Sm/^{144}Nd$-$\varepsilon_{Nd}(t)$ diagram (Fig. 4(a)) indicate that BS1 samples are probably derived from a depleted mantle source with $\varepsilon_{Nd}(t) = +6.7 — +7.4$, EC1 from an enriched mantle source with $\varepsilon_{Nd}(t) = -1.4 — -0.4$, and EC2 from a source between the two with $\varepsilon_{Nd}(t) = -2.5 — +3.2$, one sample with more sediment addition and transient with quartzite is therefore more enriched than EC1 and other samples of EC2. $\varepsilon_{Nd}(t)$ values of BS2 vary from -6.7 to -3.5. Their protoliths might be derived from a mantle source rebuilt by previous subduction(s) and the upwelling CAB magmas might have been contaminated by continental crust.

Because no matter how $\varepsilon_{Nd}(t)$ values vary from MORB to other OIB end-members the Nb/U ratios remain close to the line Nb/U = 47[19], Nb/U-$\varepsilon_{Nd}(t)$ diagram reflects the mantle characteristics of the protoliths as well as the addition of sediments (Fig. 4(b)). EC1 assemblage samples are plotted around the EM1 field, EC2 assemblage samples between EM1 and HIMU fields, indicative of their OIB provenance. Their higher NB/U ratios and thus deviation of their plots from the line Nb/U = 47 suggest that U loss occurs in the dehydration of the subducting slab. U loss is also verified by the high Th/U ra-

tios of the EC1 and EC2 samples—more than 4.2 except for sample 1054, because except for lower continental crust and eclogites, no other substances in the terrestrial globe have Th/U ratios higher than 4.2, and the addition of lower continental crust substance and eclogites into the protoliths of these two assemblages is practically impossible. BS1 samples are plotted closely under the line MORB + CC, indicating their protoliths to be a mixture of MORB and minor sediments. BS2 assemblage plots are the closest to the continental crust (CC) field, in accordance with the trace element discussion, their protoliths probably are CAB basalts derived from previous subduction triggered magmatism plus mixing sediments or simply redeposited CAB materials.

Based on the above major, trace element and Sm-Nd isotope analyses, it is concluded that the geochemical characteristics of the protoliths of the four HP-UHP rock assemblages EC1, BS1, BS2 and EC2 correlate respectively with OIB basalts, NMORB basalts, CAB basalts and EMORB basalts which are between OIB and NMORB types.

An OIB basalt is formed in a within-plate setting resulting from a mantle plume activity[19,20]; an NMORB basalt formed at a seafloor spreading center, typically a mid-ocean ridge; and an EMORB basalt formed on a seamount or at a mid-ocean ridge in the vicinity of a mantle plume[13,14]. Though the major, trace and radiogenic daughter elements reflecting geochemical characteristics of EC1, EC2 and BS1 assemblage rocks are akin to OIB, EMORB, and NMORB basalts respectively, the close correlation of their major, trace elements suggests that they share a common mantle source. In the diagrams of Ti and Zr (Fig. 5 (a), (f); Fig. 6), Nb and Zr (Fig. 5(c), (d); Fig. 6), and Ti and P (Fig. 5(b)) the plots of the three assemblage samples show pronounced correlations.

The coherent occurrence of OIB, EMORB and NMORB rocks in Ankara ophiolitic mélange, Turkey, is interpreted to be formed on a seamount[21]. A blueschist-greenschist series is formed in Fan-Karategin belt, Tajikistan, the metamorphosed alkaline basalts are geochemically akin to OIB basalts while the metamorphosed tholeiites akin to EMORB basalts. Volkova and Budanov[22] suggested that it is formed at a seamount-like structure underneath a within-plate mantle plume. Niu et al.[13] reported the coherent occurrence of basalts from highly enriched alkaline to extremely depleted tholeiitic types in several seamount settings near the east Pacific rise (EPR) and proposed that they were derived from a long-evolved heterogeneity in EPR district. Some geochemical analyses of the metavolcanics and metavolcaniclastics in the present study area show that they are akin to OIB, EMORB, and NMORB basic rocks, suggesting they are formed at a seamount setting[23].

EC1, EC2, BS1 assemblages of southwestern Tianshan HP-UHP belt, Xinjiang occur within an area of several square kilometers, EC1 and EC2 assemblages meet in the same section and BS1 assemblage is closely nearby. The coherent occurrence, together with their obvious differences and close correlation of chemical compositions, suggests that they are formed at a common seamount setting, probably derived from a small heterogeneity in the mantle.

Contrast to the above three, the field occurrence and geochemical features reflected by major, trace element and radiogenic daughter element indicate that BS2 assemblage is probably the arc CAB basalts developed by synchronous subduction-triggered magmatism, the synchron-magmatism heating began at 290 Ma[9]. The first discovered arc volcanics in the present study area provide evidence for that the paleo-Tianshan ocean was once wide-open and its closing lasts for a long period such that the previous arc volcanics are eroded, enwrapped by subducting slab and subjected to HP-UHP metamorphism in subduction zone subsequently.

5 Conclusions

(1) Geochemical characteristics of the UHP eclogites and related blueschists in southwestern Tianshan HP-UHP belt, Xinjiang indicate that they are two types of basaltic rocks formed at different tectonic settings: the oceanic basalts formed at a seamount and the arc basalts at continental margin volcanic arcs.

(2) There exist 4 types of protoliths: OIB-like meta-alkaline basalts derived from an enriched mantle source with ε_{Nd} values of -1.4 to -0.4; NMORB-like basalts from a depleted mantle source with ε_{Nd} values of $+6.7$ to $+7.4$; EMORB-like basalts from a transient mantle source with ε_{Nd} values of -2.5 to $+3.2$; and arc calc-alkaline basalts from a highly enriched mantle source with ε_{Nd} values of -6.7 to -3.5.

(3) The UHP belt is of typical UHP metamorphosed oceanic crust, and some arc volcanic substances take part in the deep subduction as the paleo-Tianshan ocean closes.

References

1 Gao J., Zhang L., Wang Z. et al. Metamorphic minerals and metamorphism evolution of western Tianshan high pressure belt. Rock and Mineral Magazine (in Chinese), 1997, 16(3): 244—254.

2 Gao J., Li M., He G. et al. Paleozoic tectonic evolution of the Tianshan Orogen, northwestern China. Tectonophysics, 1998, 287: 213—231.

3 Gao J., Klemd R., Zhang L. et al. P-T path of high pressure low temperature rocks and tectonic implications in the western Tianshan Mountains (NW China). Journal of Metamorphic Geology, 1999, 17: 621—636.

4 Zhang L. F., Ellis D. J., Williams S. et al. Ultrahigh pressure metamorphism in western Tianshan, China. Part II: Evidence from magnesite in eclogite. American Mineralogist, 2002, 87: 861—866.

5 Zhang L. F., Ellis D. J. and Jiang W. Ultrahigh pressure metamorphism in western Tianshan, China. Part I: Evidences from the inclusion of coesite pseudomorphs in garnet and quartz exsolution lamellae in omphacite in eclogites. American Mineralogist, 2002, 87: 853—860.

6 Zhang L. F., Ellis D. J. Arculus R. J. et al. Ultradeep subduction of carbonates to the mantle: evidence from the carbonate reaction of magnesite + calcite (aragonite) = dolomite in metapelites from western Tianshan, China, Journal of Metamorphic Geology, 2003, 21: 523—529.

7 Zhang L. F., Song S. G., Ai Y. L. et al. Relict coesite exsolution in omphacite from western Tianshan eclogites, China. American Mineralogist, 2005, 89: 180—186.

8 Zhang L., Gao J., Ekerbair S. et al. Low temperature eclogite facies metamorphism in Western Tianshan, Xinjiang. Science in China (Series D), 2000, 30(4): 345—354.

9 Li Q. and Zhang L. The P-T path and geological significance of lowpressure granulite-facies metamorphism in Muzhaerte, southwest Tianshan, Xinjiang, China. Acta Petrologica Sinica (in Chinese), 2004, 20(3): 583—594.

10 Zhang L., Song S., Song B. et al. SHRIMP U-Pb zircon dating of HP-UHP metamorphic rocks from Western Tianshan, China. Abstract of The Alice Wain Memorial Western Norway Eclogite Field Symposium. NGU Report, 2003, 055: 180.

11 Staudigel H., Plank T., White B. et al. Geochemical fluxes during seafloor alteration of the basaltic upper oceanic crust: DSDP sites 417 and 418. In: Subduction: Top to Bottom, American Geophysical Union , Geophysical Monograph, 1996, 19—38.

12 Becker H., Jochum K. P. and Carlson R. W. Trace element fractionation during dehydration of eclogites from high-pressure terranes and the implications for element fluxes in subduction zones. Chemical Geology, 2000, 163: 65—99.

13 Niu Y., Regelous M., Wendt I. J. et al. Geochemistry of near-EPR seamounts: importance of source vs. process and the origin of enriched mantle component. Earth and Planetary Science Letters, 2002, 199: 327—345.

14 Winchester J. A. and Floyd P. A. Geochemical magama type discrimination: application to altered and metamorphosed basic igneous rocks. Earth and Planetary Science Letters, 1976, 28: 459—469.

15 Sun S. S. and McDonough W. F. Chemical and isotopic systematics of oceanic basalts: implications for mantle composition and processes. In: Magmatism in the Ocean Basin. Geol. Soc. Spec. Publ., 1989, 42: 313—345.

16 Thompson G., Bryan W. B. and Humphris S. E. Axial volcanism of the East Pacific Rise, 10—12N. In: Magmatism in the Ocean Basin. Geol. Soc. Spec. Publ., 1989, 42: 181—200.

17 Li S. Implications of εNd-La/Nb, Ba/Nb, Nb/Th diagrams to mantle heterogeneity-classification of island arc basalts and decomposition of EM II component. Geochemistry (in Chinese), 1994, 23(2): 105—114.

18 Pearce J. A., Baker P. E., Harvey P. K. et al. Geochemical evidence for subduction fluxes, mantle melting and fractional crystallization beneath the South Sandwich Island Arc. Oceanographic Literature Review, 1996, 43(2): 155.

19 Hofmann A. W. Mantle geochemistry: the message from oceanic volcanism. Nature, 1997, 385(16): 219—229.

20 Doubleday R. A., Leat P. T., Alabaster T. et al. Allochthonous oceanic basalts within the Mesozoic accretionary complex of Alexander Island. Antarctic: remnants of proto-Pacific oceanic crust. J. Geol. Soc. (Lond.), 1994, 151: 65—78.

21 Floyd P. A. Geochemical discrimination and petrogenesis of alkalic basalt sequences in part of the Ankara melange, central Turkey. J. Geol. Soc. (Lond.), 1993, 150: 541—550.

22 Volkova N. I. and Budanov V. I. Geochemical discrimination of metabasaltic rocks of the Fan-Karategin transitional blueschist/greenschist belt, South Tianshan, Tajikistan: seamount volcanism and accretionary tectonics. Lithos, 1999, 47: 201—216.

23 Gao J. and Klemd R. Formation of HP-LT rocks and their tectonic implications in the western Tianshan Orogen, NW China: geochemical and age constraints. Lithos, 2003, 66: 1—22.